UDC:546.56.86.22

PHASE RELATIONS IN THE Cu_3SbS_4-Sb_2S_3-S SYSTEM

P.R. Mammadli[1,2], V.A. Gasimov[2], D.M. Babanly[1,2]

[1]*Azerbaijan State Oil and Industry University, French -Azerbaijani University (UFAZ)*
[2]*Acad. M. Nagiyev Institute of Catalysis and Inorganic Chemistry*
National Academy of Sciences of Azerbaijan,
H. Javid Ave. 113, Baku, AZ1143, e-mail: parvin.mammadli@ufaz.az

Received 16.12.2021
Accepted 25.02.2022

***Abstract**: Phase relations in the Cu_3SbS_4-Sb_2S_3-S system were determined experimentally over the entire concentration range by means of differential thermal analysis (DTA) and powder X-ray diffraction (PXRD) techniques. One boundary, two internal polythermal sections, and the liquidus surface projection of the system were constructed. Primary crystallization fields of existing phases, as well as, types and coordinates of non- and monovariant equilibria were determined. It was defined that, the concentration triangle under study is an independent subsystem of the Cu-Sb-S ternary system and belongs to the monotectic type with a wide stratification field of two liquids.*

***Keywords:** DTA, PXRD, phase diagram, stibnite, famatinite, immiscibility field*
DOI: 10.32737/2221-8688-2022-1-40-47

1. Introduction

Copper, antimony-based chalcogenides have been recognized as a large group of materials composed of non-hazardous, cost-effective merit elements promising for a variety of applications [1,2]. So that, sulphosalt group semiconductors such as chalcostibite ($CuSbS_2$), skinnerite (Cu_3SbS_3), famatinite (Cu_3SbS_4), tetrahedrite ($Cu_{12+x}Sb_{4+y}S_{13}$, $0 \leq x \leq 1.92$ and $0.02 \leq y \leq 0.27$) are a relatively new class of materials that can be utilized in thin-film solar cells, photoelectrochemical hydrogen production, etc. [2-5]. Among them, famatinite mineral - Cu_3SbS_4 has a simple zinc-blende related structure with a moderate band gap, which is favorable for high thermoelectric performance [6-8]. It is reported that Cu_3SbS_4 is suitable as a superabsorber material in photovoltaics because of high absorption coefficient over the visible region [9-11].

From the chalcogenide semiconductor class, stibnite (Sb_2S_3) is a continuing promising contender for applications in the most diverse electronic devices including the vidicon type of television camera tubes, microwave, switching, optoelectronic and photovoltaic devices [12-15]. It has also been proposed as a photoanode material in photocatalytic water splitting [16,17].

The study of phase relations composed of known phases possessing promising functional properties is one of the basic approaches to the design and preparation of novel advanced materials in inorganic materials science [18-23]. Taking into consideration the scientific and practical importance of the Cu-Sb-S ternary system in terms of the search for environmentally friendly, low-cost functional materials, the solid-phase equilibrium diagram of this system, and the thermodynamic properties of copper antimony sulfides were studied by us [24]. Later on, the $CuSbS_2$-Cu_3SbS_3-Sb_2S_3 and $CuSbS_2$-Sb_2S_3-S independent subsystems of this system were studied as well [25, 26].

In the present contribution, as a continuation of our investigations, we report about the phase interactions in the subsystem Cu_3SbS_4-Sb_2S_3-S (A).

Constituent phases of the subsystem (A) have been studied in detail. Sb_2S_3 melts congruently at 823 K [27] and crystallizes into orthorhombic structure (Sp.gr. P*nma*): a = 11.3107; b = 11.2285 Å; c = 3.8363 [28]. Cu_3SbS_4 known as famatinite mineral melts congruently at 908 K [29,30] and crystallizes

into tetragonal structure (Sp.gr. $I\bar{4}2m$): a = 5.391(1), c = 10.764(1) Å [31].

Two boundary quasi-binary sections of the system A have been previously studied. The phase diagram of the system Cu_3SbS_4 - Sb_2S_3 is of a simple eutectic type [25], while the system Sb_2S_3-S is characterized by the monotectic and eutectic equilibria [27].

2. Experimental part

Alloys of the system (A) were prepared from the preliminarily synthesized and identified Sb_2S_3 and Cu_3SbS_4 compounds, and elemental sulphur. Elemental copper (Cu-00029; 99.9999%), antimony (Sb-00002; 99.999%) and sulphur (S - 00001; 99.999%) of high purity from *Evochem Advanced Materials GmbH* (Germany) were used for synthesis.

Compounds were synthesized by fusion of the elemental substances in stoichiometric ratios in evacuated up to ~10^{-2} Pa and sealed quartz ampoule of the 15x1.5 cm size in a two-zone inclined furnace [24-26]. The temperature of the hot zone of the furnace was gradually increased to ~50^0C higher than the melting point of the corresponding compound within 3-4 hours, while the temperature of the upper, "cold" zone of the furnace was 650 K, which is slightly below the boiling point of sulphur (718 K [32]). The synthesis was continued in this mode for the next 3-4 hours and the ampoules were completely transferred into the hot zone. The resulting liquids were mixed by shaking the alloys and the oven was gradually cooled. After synthesis, the ampoules were kept at 750 K for 100 h.

The identity of the synthesized compounds was monitored by differential thermal analysis (DTA) and powder X-ray diffraction (PXRD) methods, obtained data well coincided with the literature [27-31].

Two sets of samples (0.5 g by mass each) were prepared by co-melting of different proportions of the preliminarily synthesized compounds in evacuated quartz ampoules. Because of the presence of elemental sulphur in the alloys of the Cu_3SbS_4-S section and Cu_3SbS_4-Sb_2S_3-S concentration triangle, during the synthesis and analysis of these alloys by the DTA method, we used specially designed thick-walled (~2.5 cm) transparent quartz ampoules. The Interior diameter of ampoules was 5-6 mm, length – 25-30 sm. In this case, the empty volume inside the ampoule doesn't exceed 500 mm^3 (0.5 cm^3), which in turn allows to keep the composition of alloys constant during heating due to the evaporation of sulphur. After synthesis, alloys were annealed at 500 K for ~100 hours, then at 370K for 20 hours.

Obtained equilibrium samples were examined by DTA and PXRD methods. DTA of the samples was carried out in evacuated quartz ampoules on a differential scanning calorimeter of the 404 F1 Pegasus System (NETZSCH). NETZSCH Proteus Software was used to process the results of measurements. The accuracy of the temperature measurements was within $\pm 2^{0}$. X-ray analysis was carried out at room temperature on the Bruker D2 PHASER diffractometer with $CuK\alpha_1$ radiation. Topas 4.2 Software was used to index obtained diffraction patterns.

3. Results and discussion

Compositions of alloys are expressed in equal numbers of atoms using the corresponding coefficients in front of their formulas on the phase diagram of the system (A) and its various sections. This is identical to the expression of composition in atomic percent and allows this data to be used in the general phase diagram of the Cu-Sb-S system without recalculation of composition.

3.1. 0.125Cu_3SbS_4 – S quasi-binary boundary system (Fig.1)

As it can be seen from the T-x diagram constructed based on the DTA results (Fig.1), the system Cu_3SbS_4 – S is characterized by monotectic and eutectic equilibrium degenerated near elemental sulphur. The immiscibility area at the monotectic equilibrium temperature (896K) occupies a wide (~5-99 at % el. S) concentration range. Eutectic composition Cu_3SbS_4 + S crystallizes at 390K.

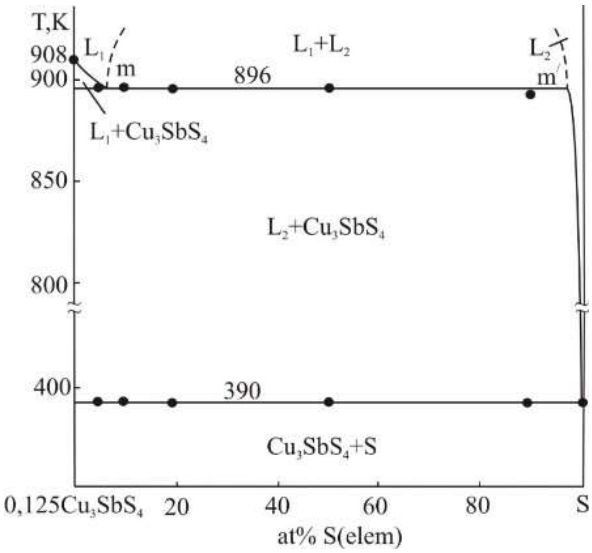

Figure 1. The T-x phase diagram of the system Cu_3SbS_4-S

XRD results prove constructed T-x diagram of the system Cu_3SbS_4-S. As can be seen from Fig.2, the PXRD spectrum of the 50 mol% Cu_3SbS_4 alloy is composed of the diffraction lines of Cu_3SbS_4 and elemental sulphur.

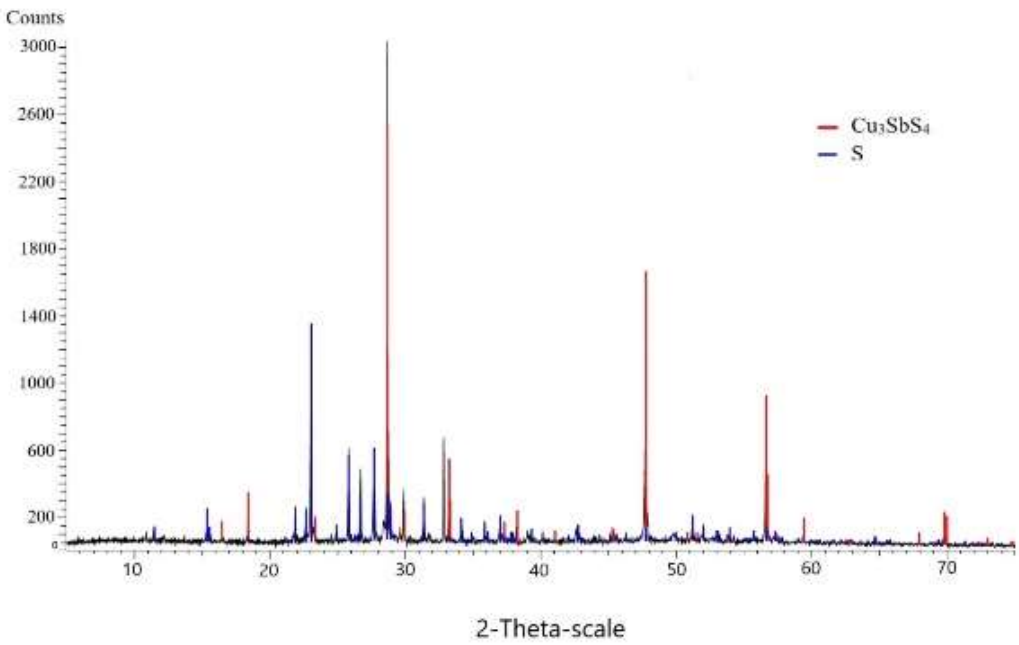

Fig. 2. PXRD spectrum of the 50 mol% Cu_3SbS_4 + 50 mol% el. S alloy

3.2. Projection of the liquidus surface of the system A (Fig.3)

Projection of the liquidus surface of the system A on the concentration triangle is given in Fig. 3. Concentration triangle Cu_3SbS_4-Sb_2S_3-S is an independent subsystem and characterized by monotectic and eutectic equilibriums. Equilibria near the sulphur corner of the concentration triangle are presented on a large scale. There is a stratification field (L_1+L_2) of two liquids ($m_1m_2m_2^{/}m_1^{/}$) in a wide concentration interval. This immiscibility field

is located in the primary crystallization areas of the famatinite (area 1) and stibnite (area 2) dividing them into 2 parts. The primary crystallization area of an elemental sulphur (area 3) occupies a small region near the S corner of the liquidus surface (Fig.3).

Liquidus surfaces of phases are limited by the e_1E, e_2E, and e_3E eutectic curves. These curves converge in the triple eutectic point E at ~390K (Fig.3). Nonvariant and monovariant equilibria of the system A are given in the table.

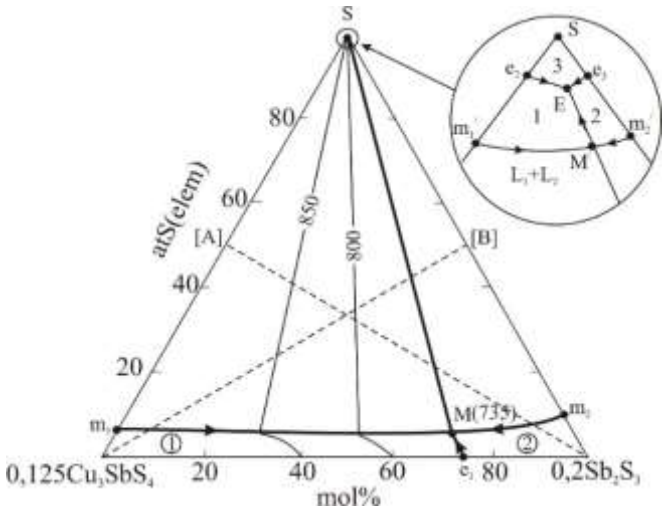

Fig. 3. Projection of the liquidus surface of the system A. Primary crystallization areas: 1– Cu_3SbS_4, 2 – Sb_2S_3, 3 – S. Dotted lines are studied polythermal sections of the system A

Table. Nonvariant and monovariant equilibria in the system Cu_3SbS_4-Sb_2S_3-S

Point or curve in the Fig.3	Equilibria	Temperature, K
e_1	$L \leftrightarrow Cu_3SbS_4 + Sb_2S_3$	745
e_2^*	$L \leftrightarrow Cu_3SbS_4 + S$	390
e_3^*	$L \leftrightarrow Sb_2S_3 + S$	383
E*	$L \leftrightarrow Cu_3SbS_4 + Sb_2S_3 + S$	381
$m_1(m_1^/)$	$L_1 \leftrightarrow L_2 + Cu_3SbS_4$	896
$m_2(m_2^/)$	$L_1 \leftrightarrow L_2 + Sb_2S_3$	803
$MM^/$	$L_1 \leftrightarrow L_2 + Cu_3SbS_4 + Sb_2S_3$	735
e_1M	$L_1 \leftrightarrow Cu_3SbS_4 + Sb_2S_3$	745-735
$M^/E^*$	$L_2 \leftrightarrow Cu_3SbS_4 + Sb_2S_3$	735-381
$m_1M(m_1^/M^/)$	$L_1 \leftrightarrow L_2 + Cu_3SbS_4$	896-735
$m_2M(m_2^/M^/)$	$L_1 \leftrightarrow L_2 + Sb_2S_3$	803-735
$e_2^*E^*$	$L \leftrightarrow Cu_3SbS_4 + S$	390-381
$e_3^*E^*$	$L \leftrightarrow Sb_2S_3 + S$	383-381

Note: degenerated equilibria near elemental Sulphur are given with asterisk.

3.3. Polythermal sections of the system A (Fig.4 a,b)

Two polythermal sections of the phase diagram of the system A are given below (Fig.4 a,b) and analyzed in context with the projection of the liquidus surface (Fig.3). Here, [A] and [B] are 1:1 mix ratios of the constituent substances of the $0.125Cu_3SbS_4$-S and $0.2Sb_2S_3$-S boundary binary systems, consequently.

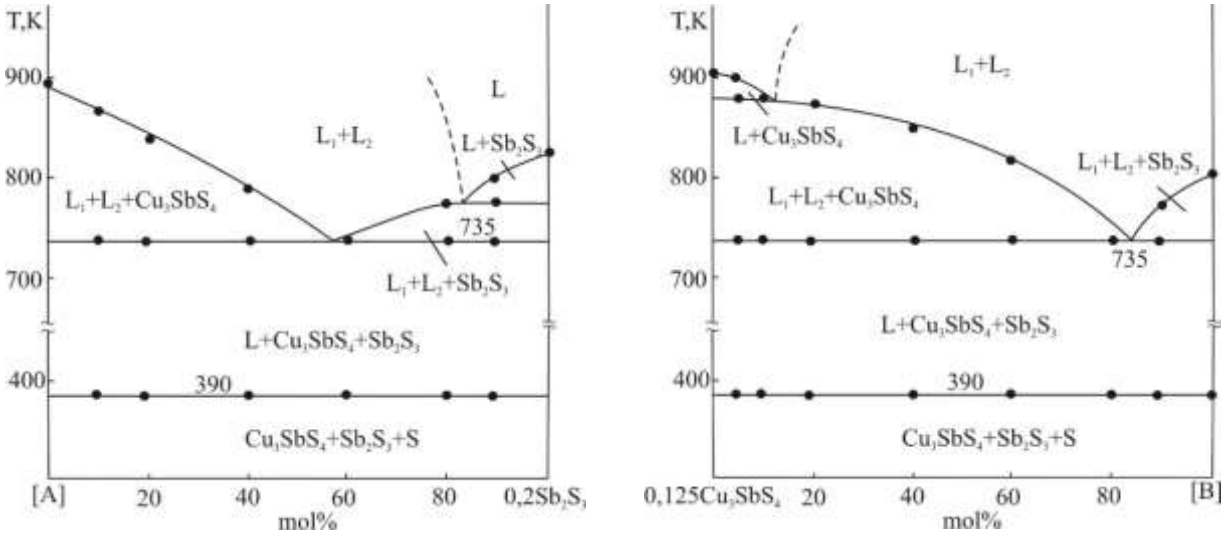

Fig. 4. T-x phase diagrams of the systems $0.2Sb_2S_3$- [A] (a) and $0.125Cu_3SbS_4$-[B] (b)

0.2 Sb_2S_3- [A] polythermal section (Fig.4a).

There is a wide (~ 85 mol%) immiscibility region of two liquid phases (L_1+L_2) along this polythermal section. Cu_3SbS_4 primarily crystallizes from this two-phase region at the ~0-60 mol% Sb_2S_3 concentration interval by the monovariant monotectic reaction $L_1 \leftrightarrow L_2 + Cu_3SbS_4$. Sb_2S_3 crystallizes in the area rich in Sb_2S_3 (>80 mol%) from one-phase liquid, and then from the L_1+L_2 two-phase area by monotectic reaction $L_1 \leftrightarrow L_2 + Sb_2S_3$. The isothermal line at 735 K belongs to the nonvariant monotectic equilibrium (Table MM/). Crystallization in the system ends by the formation of the ternary eutectic mixture Cu_3SbS_4+Sb_2S_3+S at 390K (Fig.4a).

0.125 Cu_3SbS_4 - [B] polythermal section (Fig.4b).

Crystallization processes along this polythermal section are qualitatively similar to the ones in the previous system. The difference is that here the initial crystallization of the Cu_3SbS_4 compound occurs in a small (~ 12 mol%) concentration interval from the one-phase liquid L, and in a wide concentration interval (~70 mol%) from the L_1+L_2 immiscibility area by monovariant reaction (Fig.4b). Moreover, Sb_2S_3 crystallizes in a small composition interval from the immiscibility area.

Thus, a comparative analysis of all elements of the phase diagram (Fig. 1,3,4) indicates their compatibility with each other. Presented results can be used to prepare phases based on the primary constituents of the system A, as well as their eutectic composites.

Conclusion

For the first time, the nature of the physicochemical interaction of the stibnite, famatinite minerals, and elemental sulphur was determined using DTA and powder X-ray methods. The phase diagram of the Cu_3SbS_4 – S boundary system, 2 isopleth sections, as well as, the projection of the liquidus surface of the Cu_3SbS_4-Sb_2S_3-S system were constructed. It was established that the system is of eutectic and monotectic type and characterized by the formation of a wide immiscibility area L_1+L_2 of two liquid phases.

References

1. Peccerillo E., Durose K. Copper–antimony and copper–bismuth chalcogenides—Research opportunities and review for solar photovoltaics. *MRS Energy & Sustainability*. 2018, vol. 5, no. 9, pp. 1-59. doi.org/10.1557/MRE.2018.10
2. Lei H., Chen J., Tan Z., Fang G. Review of Recent Progress in Antimony Chalcogenide Based Solar Cells: Materials and Devices. *Solar RRL*. 2019, 1900026. https://doi.org/10.1002/solr.201900026
3. Suehiro S., Horita K., Yuasa M., Tanaka T., Fujita K., Ishiwata Y., Shimanoe K., Kida T. Synthesis of Copper–Antimony-Sulfide Nanocrystals for Solution-Processed Solar Cells. *Inorganic Chemistry*. 2015, vol. 54, no. 16, pp. 7840-7845. https://doi.org/10.1021/acs.inorgchem.5b00858
4. Welch A.W., Baranowski L.L., de Souza Lucas F.W., Toberer E.S., Wolden C.A., Zakutayev A. Copper antimony chalcogenide thin film PV device development. 2015 IEEE 42nd Photovoltaic Specialist Conference (PVSC). 2015, pp. 1-4, https://doi.org/10.1109/PVSC.2015.7356357
5. Lucas F.W.S.L., Welch A.W., Baranowski L.L., Dippo P.C., Hempel H., Unold Th., Eichberger R., Blank B., Rau U., Mascaro L.H., Zakutayev A. Effects of Thermochemical Treatment on $CuSbS_2$ Photovoltaic Absorber Quality and Solar Cell Reproducibility. *The Journal of Physical Chemistry* C. 2016, vol. 120, no. 33, pp. 18377-18385. https://doi.org/10.1021/acs.jpcc.6b04206
6. Suzumura A., Watanabe M., Nagasako N., Asahi R. Improvement in Thermoelectric Properties of Se-Free Cu_3SbS_4 Compound . *Journal of Electronic Materials*. 2014, vol. 43, no. 6, pp. 2356-2361. https://doi.org/10.1007/s11664-014-3064-y
7. Lee GE., Pi JH., Kim IH. Preparation and Thermoelectric Properties of Famatinite Cu_3SbS_4 *Journal of Electronic Materials*. 2020, vol. 49, pp. 2781–2788. https://doi.org/10.1007/s11664-019-07765-8
8. Wang Q., Li J., Li J. Enhanced thermoelectric performance of Cu_3SbS_4 flower-like hierarchical architectures composed of Cl doped nanoflakes via an in situ generated CuS template *Physical Chemistry Chemical Physics*. 2018, vol. 20, №3, pp.1460–1475. https://doi.org/10.1039/C7CP06465A
9. Albuquerque G. H., Kim K-J., Lopez J. I., Devaraj A., Manandhar S., Liu Y-S., Guo J., Chang Ch-H., Herman G.S. Multimodal characterization of solution-processed Cu_3SbS_4 absorbers for thin film solar cells. *Journal of Materials Chemistry* A. 2018, vol. 6, no. 18, pp. 8682–8692. https://doi.org/10.1039/C8TA00001H
10. Van Embden J., Latham K., Duffy N. W., Tachibana Y. Near-Infrared Absorbing $Cu_{12}Sb_4S_{13}$ and Cu_3SbS_4 Nanocrystals: Synthesis, Characterization, and Photoelectrochemistry. *Journal of the American Chemical Society*. 2013, vol. 135, no. 31, pp. 11562–11571. https://doi.org/10.1021/ja402702x
11. Chalapathi U., Poornaprakash B., Park S.-H. Growth and properties of Cu_3SbS_4 thin films prepared by a two-stage process for solar cell applications. *Ceramics International*. 2017, vol. 43, no. 6, pp.5229–5235. https://doi.org/10.1016/j.ceramint.2017.01.048
12. Wu W., Shan B., Feng K., Nan H. Resistive switching behavior of Sb_2S_3 thin film prepared by chemical bath deposition. *Materials Science in Semiconductor Processing*. 2016. vol. 44, pp. 18–22. https://doi:10.1016/j.mssp.2015.12.031
13. Kim D.-H., Lee S.-J., Park M.S., Kang J.-K., Heo J.H., Im S.H., Sung, S.-J. Highly reproducible planar Sb_2S_3 -sensitized solar cells based on atomic layer deposition. *Nanoscale*. 2014, vol. 6, no. 23, pp.14549–14554. https://doi.org/10.1039/C4NR04148H
14. Salin V. I. Estimation of photodetector sensitivity in applied television systems.

Optical Engineering. 1998, vol. 37, no. 7, pp. 2091-2094. https://doi.org/10.1117/1.601731

15. Gil E. K., Lee S.-J., Sung S.-J., Cho K.Y., Kim D.-H.. Spin-Coating Process of an Inorganic Sb_2S_3 Thin Film for Photovoltaic Applications . *Journal of Nanoscience and Nanotechnology*. 2016, vol. 16, no. 10, pp. 10763–10766. https://doi.org/10.1166/jnn.2016.13235
16. DeAngelis A.D., Kemp K.C., Gaillard N., Kim K.S. Antimony(III) Sulfide Thin Films as a Photoanode Material in Photocatalytic Water Splitting. *ACS Applied Materials & Interfaces*. 2016, vol. 8, no. 13, pp. 8445–8451. https://doi.org/10.1021/acsami.5b12178
17. Wang Y-C., Zeng Y-Y., Li L-H., Qin C., Wang Y-W., Lou Z-R., Liu F-Y., Ye Z-Z, Zhu L-P. Stable and efficient photocathode using Sb_2S_3 absorber in near-neutral electrolyte for water splitting. *ACS Applied Energy Materials*. 2020, vol. 3, no. 7, pp. 6188-6194. https://doi.org/10.1021/acsaem.0c00210
18. Babanly M.B., Chulkov E.V., Aliev Z.S., Shevelkov A.V., Amiraslanov I.R. Phase diagrams in materials science of topological insulators based on metal chalcogenides. *Russ. J. Inorg. Chem.* 2017, vol. 62, no. 13, pp. 1703–1729. https://doi.org/10.1134/S0036023617130034
19. Babanly M.B., Mashadiyeva L.F., Babanly D.M., Imamaliyeva S.Z., Tagiev D.B., Yusibov Yu.A. Some issues of complex studies of phase equilibria and thermodynamic properties in ternary chalcogenide systems involving EMF measurements (review). *Russ. J. Inorg. Chem*. 2019, vol. 64, no. 13. pp. 1649-1671. https://doi.org/10.1134/S0036023619130035
20. Babanly D.M., Tagiyev D.B. Physicochemical aspects of ternary and complex phases development based on thallium chalcohalides. *Chemical Problems.* 2018, vol. 16, no. 2, pp.153-177.
21. Mashadieva L.F., Gasanova Z.T., Yusibov Yu.A., Babanly M.B. Phase equilibria in the Cu–Cu_2Se–As system. *Russian Journal of Inorganic Chemistry*. 2017, vol. 62, no. 5, pp. 598–603. https://doi.org/10.1134/S0036023617050126
22. Gasanova Z.T., Aliev Z.S., Yusibov Yu.A., Babanly M.B. Phase equilibria in the Cu-Cu_2S-As system. *Russian Journal of Inorganic Chemistry*. 2012, vol. 57, no. 8, pp. 1158–1162. https://doi.org/10.1134/S0036023612050075
23. Mashadieva L.F., Gasanova Z.T., Yusibov Yu.A., Babanly M.B. Phase Equilibria in the Cu_2Se–Cu_3AsSe_4–Se System and Thermodynamic Properties of Cu_3AsSe_4. *Inorganic Materials*. 2018, vol. 54, no. 1, pp. 8–16. https://doi.org/10.1134/S0020168518010090
24. Mashadiyeva L.F., Mammadli P.R., Babanly D.M., Ashirov G.M., Shevelkov A.V., Yusibov Yu.A. Solid-Phase Equilibria in the Cu-Sb-S System and Thermodynamic Properties of Copper-Antimony Sulfides. *JOM*. 2021, vol. 73, pp. 1522–1530. https://doi.org/10.1007/s11837-021-04624-y
25. Mammadli P.R., Mashadiyeva L.F., Gasimov V.A., Dashdiyeva G.B., Babanly D.M. Phase relations in $CuSbS_2$-Cu_3SbS_4-Sb_2S_3 system. *Azerbaijan Journal of Chemical News*. 2021, vol. 3, no. 1, pp.100-108.
26. Mammadli P.R., Gasimov V.A., Mashadiyeva L.F., Babanly D.M. Phase relations in the $CuSbS_2$-Sb_2S_3-Sb system. *JOMARD*. 2021 (accepted in print).
27. Massalski T.B., Okamoto H., Subramanian P.R., Kacprzak L. Binary alloy phase diagrams. Materials park, Ohio: ASM International, 2nd ed., 1990. vol. 3. 3589 p. https://doi.org/10.1002/adma.19910031215
28. Bayliss P., Nowacki W. Refinement of the crystal structure of stibnite, Sb_2S_3. *Z. Kristallogr*. 1972, vol. 135, pp. 308-315. https://doi.org/10.1524/zkri.1972.135.3-4.308
29. Skinner B.J., Luce F.D., Makovicky E. Studies of the Sulfosalts of Copper III; Phases and Phase Relations in the System

Cu—Sb—S. *Economic Geology*. 1972, vol. 67, no. 7, pp. 924–938. http://dx.doi.org/10.2113/gsecongeo.67.7.924
30. Babanly M.B., Yusibov Yu.A., Abishev V.T. Ternary chalcogenides on the base of copper and silver Baku: BGU Publ., 1993. 342 p. (In Russian).
31. Pfitzner A., Reiser S. Refinement of the crystal structures of Cu_3PS_4 and Cu_3SbS_4 and a comment on normal tetrahedral structures. *Zeitschrift für Kristallographie - Crystalline Materials*. 2002, vol. 217, no. 2, pp. 51-54. https://doi.org/10.1524/zkri.217.2.51.20632
32. Emsley J. The elements. New York: Oxford University Press, 3rd ed., 1998. 300 p.

Cu_3SbS_4-Sb_2S_3-S SİSTEMİNDƏ FAZA ÇEVRİLMƏLƏRİ

P.R. Məmmədli[1*], V.A. Qasımov[2], D.M. Babanlı[1,2]

[1]Azərbaycan Dövlət Neft və Sənaye Universiteti, Azərbaycan-Fransız Universiteti (UFAZ)
[2]Kataliz və Qeyri-üzvi Kimya İnstitutu, Azərbaycan Milli Elmlər Akademiyası
AZ1143, Bakı şəh., H.Cavid pr., 113; e-mail: parvin.mammadli@ufaz.az

Xülasə: *Cu_3SbS_4-Sb_2S_3-S sistemində faza tarazlıqları tam qatılıq intervalında diferensial termal analiz (DTA) və rentgen-faza analizi (RFA) üsulları ilə tədqiq edilmişdir. Sistemin bir sərhəd, iki daxili politermik kəsiyi və likvidus səthinin proyeksiyası qurulmuşdur. Mövcud fazaların ilkin kristallaşma sahələri, nonvariant və monovariant tarazlıqların tipləri və koordinatları təyin edilmişdir. Müəyyən olunmuşdur ki, tədqiq olunan qatılıq üçbucağı Cu-Sb-S üçlü sisteminin müstəqil alt sistemi olub geniş təbəqələşmə sahəsinə malik monotektik tipli faza diaqramı əmələ gətirir.*
Açar sözlər: *DTA, RFA, faza diaqramı, stibnit, famatinit, təbəqələşmə sahəsi*

ФАЗОВЫЕ РАВНОВЕСИЯ В СИСТЕМЕ Cu_3SbS_4-Sb_2S_3-S

П.Р. Маммадли[1 *],В.А. Гасымов[2], Д.М. Бабанлы[1,2]

[1] Азербайджанский государственный университет нефти и промышленности, Азербайджано-Французский университет (UFAZ)
[2]Институт катализа и неорганической химии Национальной АН Азербайджана
Пр. Г. Джавида, 113, Баку, AZ1143; e-mail: parvin.mammadli@ufaz.az

Аннотация: *Фазовые равновесия в системе Cu_3SbS_4-Sb_2S_3-S в полном диапазоне концентраций были исследованы методами дифференциального термического (ДТА) и рентгенофазового анализов (РФА). Построены одно граничное и два внутренних политермических сечения, а также проекция поверхности ликвидуса системы. Определены поля первичной кристаллизации существующих фаз, типы и координаты нон- и моновариантных равновесий. Установлено, что исследуемый концентрационный треугольник является самостоятельной подсистемой тройной системы Cu-Sb-S и относится к монотектическому типу с широкой областью расслаивания двух жидкостей.*
Ключевые слова: *ДТА, РФА, фазовая диаграмма, стибнит, фаматинит, область расслаивания*